

NONLINEAR OPTICAL PHENOMENA

PACS numbers: 42.65.Dr; 42.70.Jk; 42.55.Mv
DOI: 10.1070/QE2011v041n10ABEH014586

Stimulated resonance Raman scattering from organic dyes in a multiple-scattering medium as a potential method for determining their vibrational spectra

V.P. Yashchuk, E.A. Tikhonov, A.O. Bukatar', O.A. Prigodiuk, A.P. Smaliuk

Abstract. **A method is described for deriving Raman spectra of organic dyes from their random lasing spectra. The method was tested using Rhodamine 6G. The Raman spectrum obtained for this dye agrees well with the spectra measured by standard techniques but is more structured, which allows unresolved features to be detected. The spectrum provides more detailed information owing to the interference between the Raman scattered light and amplified spontaneous emission of the dye molecules within a photon mean free path. One advantage of the method is that the luminescence of the dye helps to observe Raman lines, which allows one to work in the Stokes region and facilitates the measurement procedure.**

Keywords: *stimulated resonance Raman scattering, random lasing, Raman spectrum, organic dye, multiple-scattering media, vesicular films, amplified spontaneous emission.*

1. Introduction

Raman spectra of organic dyes are difficult to measure because of their strong luminescence: the Raman signal is less than 0.01% of the luminescence intensity. This problem can be obviated using several rather complex techniques, the most widespread of which is surface enhanced resonance Raman scattering (SERRS) [1, 2]. In this technique, test molecules are placed on a rough metallic surface or metallic nanoparticles, which ensures a considerable increase in Raman scattering probability. However, for the emission to be dominated by surface molecules, extremely low analyte concentrations should be used, which dramatically reduces the signal and requires sensitive detection techniques.

Raman spectra can also be obtained using inverse Raman scattering. Raman lines then have the form of dips in the continuous spectrum of probe light in the anti-Stokes region, where no luminescence occurs [3]. This method requires two synchronised high-intensity light sources, one monochromatic and the other with a continuous spectrum. A rather complex technique is coherent anti-Stokes Raman spectroscopy (CARS) [4], which requires at least two synchronised lasers, one of which should allow gradual lasing frequency tuning.

V.P. Yashchuk, A.O. Bukatar', O.A. Prigodiuk, A.P. Smaliuk Department of Physics, Taras Shevchenko Kyiv National University, Vladimirskaya ul. 64, 01601 Kyiv, Ukraine; e-mail: yavasil@ukr.net;
E.A. Tikhonov Institute of Physics, National Academy of Sciences of Ukraine, prosp. Nauki 46, 03028 Kyiv, Ukraine

Received 14 March 2011; revision received 28 July 2011
Kvantovaya Elektronika **41** (10) 875–880 (2011)
Translated by O.M. Tsarev

Recent work [5, 6] has shown that, in multiple-scattering (MS) active media, Raman lines of dyes may emerge in so-called random lasing (RL) spectra. RL is due to the fact that, when light propagation in a medium is diffuse, the gain and optical loss are proportional to the active region volume and surface area, respectively. Therefore, extending the active region (raising the pump power), one can reach a gain exceeding the loss and, hence, photon multiplication in the medium [7]. Increasing the residence time of a photon in the active medium, multiple scattering ensures positive feedback, which is nonresonant and uses only intensity in the case of diffuse light propagation [8, 9]. In the diffusive regime, which takes place under conditions typical of MS media, $\bar{l}_m \gg \bar{l}_f \gg \lambda$ (where $\bar{l}_m$, $\bar{l}_f$ and λ are a characteristic length scale of the medium, the photon mean free path and the wavelength, respectively), scattered waves are incoherent, the influence of interference is insignificant, and the stimulated emission spectrum is continuous. However, its width and especially the dynamics of its narrowing with increasing pump power are similar to those in homogeneous organic dye laser media [10]. This suggests that there is lasing in arbitrary directions along random scattered light trajectories. Such lasing is referred to as random.

High-intensity RL emission contributes to the development of stimulated Raman scattering (SRS), which shows up at all the Raman frequencies that fall within the RL spectrum [6, 11]. According to recent work [11], this dual process can be thought of as a special case of CARS, in which a second component of bichromatic pumping – RL emission at Stokes frequencies – is generated directly in the medium. This mechanism accounts for all the observed features of this effect. In particular, the above-mentioned manifestation of all the Raman frequencies is due to the continuous spectrum of this component. Note that, for the process to occur, it is only necessary that Stokes Raman lines fall within the RL spectrum (the effective gain band of the dye in the MS medium). As a consequence, the effect is most pronounced in highly efficient laser dyes, as confirmed by experiment. This distinguishes it from stimulated resonance scattering from excited states, which depends crucially on the broadening and lifetime of excited states of the dye molecule [12] and, in addition, requires that the scattered light be in resonance with the luminescence. Therefore, the effect should take place throughout the luminescence spectrum of the dye, rather than within the gain band.

The above processes lead to an RL spectrum that comprises two components differing in emission mechanism and spectrum: one component has a broad, continuous spectrum ($\Delta\lambda$ = 7–20 nm) due to stimulated emission from the dye molecules, and the other has a quasi-discrete spectrum, with relatively narrow lines due to SRS. These processes occur in

parallel and influence one another, resulting in a quasi-discrete spectrum.

Using this spectrum, one can find the Raman spectrum. In this paper, based on the above mechanism of RL in dyes, we develop and test a technique for determining their Raman spectrum.

2. Technique for determining Raman spectra from RL spectra

To adequately find a Raman spectrum from an RL spectrum, one should take into account the mutual influence of stimulated emission and SRS because the contributions of these processes to the emission intensity at a Raman frequency are due to the common field at this frequency. Under the assumption that the stimulated emission and SRS intensities add up, their contributions to the total emission intensity at the Raman frequency are represented by differential equations that describe light amplification as a result of stimulated emission and scattering processes [11]. The RL intensity, $I_{RL}(\omega)$, can then be represented in the form

$$I_{RL}(\omega) = I_{lum}(\omega)\, G_{se}(\omega)\, G_{ss}(\omega), \qquad (1)$$

where $I_{lum}(\omega)$ is the spectral distribution of the spontaneous emission (luminescence) intensity, and $G_{se}(\omega)$ and $G_{ss}(\omega)$ are the spectral distributions of the gains due to stimulated emission and SRS, respectively.

Note that the two types of radiation, generated over a mean free path, are coherent with one another, so the fields of these partial waves should add up. However, in the case of diffuse light propagation through an MS medium, the coherence is disturbed by every elastic scattering event. Therefore, the sum radiation of either type and the total radiation should result from the addition of intensities, like in the case of nonresonant feedback [7, 8].

The first two factors in (1) are responsible for the continuous spectrum of amplified spontaneous emission (ASE), which has the form of a background in the RL spectrum, and the third factor describes SRS, responsible for the line component. $G_{ss}(\omega)$ can be expressed through third-order nonlinear susceptibility, $\chi^{(3)}_{srs}(\omega)$, related to SRS:

$$G_{ss}(\omega) = \exp[\chi^{(3)}_{srs}(\omega) I_p \bar{l}], \qquad (2)$$

where I_p is the pump intensity and $\bar{l}$ is the photon mean free path in the MS medium. In view of (2), the Raman spectrum can be thought of as a spectral dependence of the nonlinear susceptibility $\chi^{(3)}_{srs}(\omega)$, which is given by

$$\chi^{(3)}_{srs}(\omega) = \ln\{I_{RL}(\omega)/[I_{lum}(\omega)\, G_{se}(\omega)]\}. \qquad (3)$$

In this formula, the numerator and denominator represent the spectral dependences that can be found experimentally: the RL spectrum and its continuous background. Therefore, Eqn (3) suggests an algorithm for finding a Raman spectrum from an RL spectrum. It includes the evaluation of the continuous background, $I_b(\omega)$, i.e. the denominator in (3), $I_{lum}(\omega)\, G_{se}(\omega)$, in the measured quasi-discrete spectrum $I_{RL}(\omega)$ and subsequent mathematical operations according to (3).

The described algorithm stems logically from the mechanism of the phenomenon [6, 11] and reflects the general trend found experimentally that the emission intensity $I_{RL}(\omega_s)$ of a Raman line at frequency ω_s is proportional to the background intensity at this frequency, $I_b(\omega_s)$. Therefore, to find the true intensity distribution of Raman lines, one should divide the RL spectrum by its background, as reflected by Eqn (3).

It is worth noting that, because $I_{RL}(\omega_s)$ is proportional to $I_b(\omega_s)$, strong luminescence helps Raman lines to show up, in contrast to other methods. For this reason, in contrast to inverse Raman scattering [3] and CARS [4], the Raman spectrum is here measured in the Stokes region, which simplifies the measurement procedure.

To take into account interference between the types of secondary emission under consideration within a mean free path, one should consider not differential equations in terms of intensities [11] but a shortened wave equation, in which the influence of stimulated emission and scattering is taken into account through complex dielectric permittivity and third-order polarisability. It can be shown that the spectrum is then described by an expression similar to (1), but the sign of third-order nonlinearity changes at a Raman resonance frequency, which makes the shape of the spectral line similar to that in CARS [4]. This has no dramatic effect on the described technique for determining a Raman spectrum from an RL spectrum but allows finer spectral features considered below to be explained.

3. Results and discussion

The technique described above was used to measure and analyse Raman spectra of two organic laser dyes (Fig. 1): Rhodamine 6G (R6G) and polymethine dye 920 (P920).

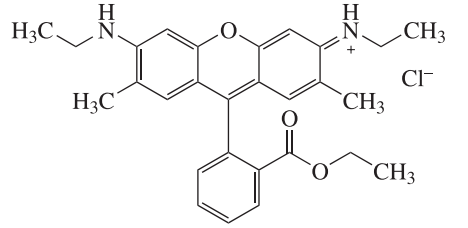

R6G

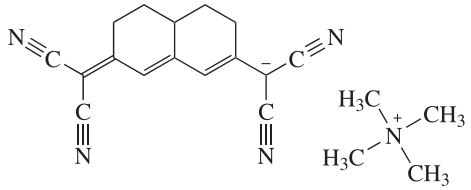

P920

Figure 1. Structural formulas of the R6G and P920 molecules.

The Raman spectrum of R6G was measured earlier using standard techniques [1–3], whereas the Raman spectrum of P920 has not yet been reported. R6G was introduced into a polymer film about 15 μm thick on a Lavsan substrate. UV irradiation of the polymer film produced densely packed nitrogen vesicles of mean diameter $\bar{d}$ = 1.2 μm [5]. Owing to the dense packing of the vesicles, their considerable relative index of refraction in the polymer (n = 1.5), the relation $\bar{d} > \lambda$ and the high dye concentration (C_d = (3–5)×10^{-3} M), such film is an effective MS active medium with diffuse light propagation and a low RL threshold.

In the case of P920, because of its low photochemical stability in vesicular films we used an MS medium in the form of a solid suspension of borazon dielectric particles (mean diameter, 2 μm) in polyurethane acrylate. The solid suspension was prepared through rapid photopolymerisation of an ethanolic solution of the dye and polyurethane acrylate, which allowed us to avoid significant inhomogeneity of the material because of sedimentation. Owing to the nearly close packing of the particles in the suspension, their high relative index of refraction in the polymer ($n = 1.6$) and the other factors indicated above, the suspension was also an effective MS active medium with diffuse light propagation and a fairly low RL threshold.

Measurements were made at liquid helium temperature (8 K), where the Raman lines in the RL spectrum were best seen. This was due to two factors: the narrowing of the Raman lines and the better coincidence of the ASE background (the continuous component of RL) with the spectral region of the Raman lines. Because the ASE band is substantially narrower than the Raman spectrum of the dye, the spectrum was obtained by scanning the ASE band along the spectral axis through variations in dye and vesicle concentrations.

The films were pumped by a frequency-doubled Q-switched Nd:YAG laser. The pump intensity was varied from 3 to 20 MW cm^{-2}. Emission spectra were acquired in one pulse using a CCD array/diffraction grating spectrograph with a spectral resolution of 0.3 nm. Whether the line component of the RL spectra was due to Raman scattering was ascertained using a tunable Nd:phosphate glass laser: the spectral lines of the two dyes were shifted along the spectral axis according to the pump frequency. The behaviour of the spectral lines of the two dyes corresponded to typical properties of SRS in combination with stimulated emission of dye molecules [6, 11]: they showed up only within the spectral range of the continuous component of RL and their intensity increased superlinearly with pump intensity.

Figure 2 shows the measured RL spectrum of R6G, its continuous and line components, and the SERRS spectrum of R6G reported in Ref. [1]. For comparison with the line component, the SERRS spectrum is displaced to the visible region and converted to wavelengths $\lambda = (\nu_e - \nu_s)^{-1}$, where ν_e and ν_s are the excitation frequency and Raman shift in the SERRS spectrum. There is good agreement between the frequencies of the SERRS lines and those of the line component of RL, but their relative intensities differ markedly.

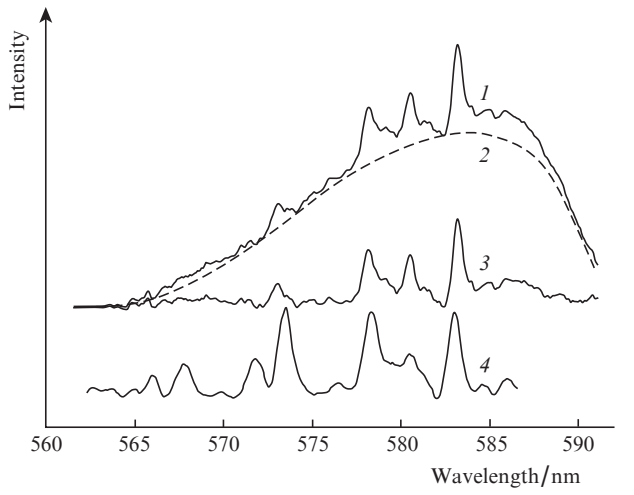

Figure 2. (*1*) Quasi-discrete RL spectrum of R6G, its (*2*) continuous and (*3*) line components, and (*4*) SERRS spectrum of R6G [1].

Figure 3 shows the Raman spectrum derived from the RL spectrum of R6G using the algorithm defined by (3). For convenience, it will be referred to as the Raman–RL spectrum. In Fig. 2, this spectrum is compared to the SERRS spectra measured by two groups [1, 2]. The Raman–RL spectrum of R6G is seen to be similar to its spontaneous Raman spectra [1, 2]: there is not only agreement between Raman frequencies but also good correlation between intensities. An essential point is that the intensities correlate only when the above algorithm is applied to the RL spectra, whereas the line component as such [Fig. 2, spectrum (*3*)] does not represent the actual Raman intensities. This indicates that the described algorithm allows one to adequately find a Raman spectrum from an RL spectrum.

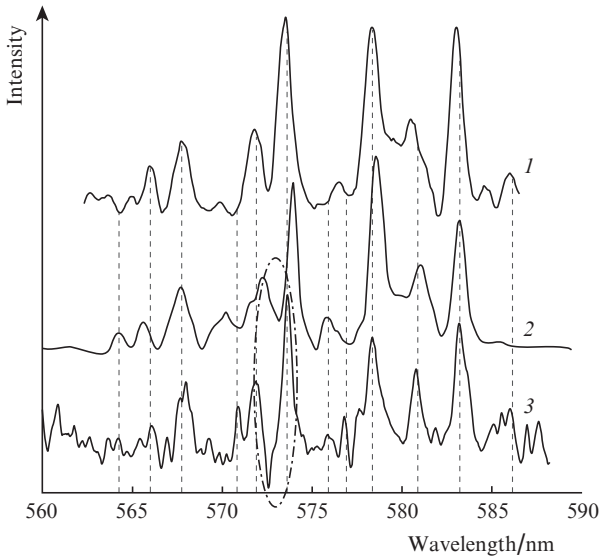

Figure 3. (*1*, *2*) SERRS spectra of R6G from Refs [1, 2], respectively, and (*3*) Raman–RL spectrum of R6G.

At the same time, the Raman–RL spectrum shows more features in comparison with the SERRS spectra and has sharper, better resolved spectral lines. An instructive example is provided by the decomposition of these spectra into elementary Gaussian components in the range 577–584 nm (Fig. 4). As seen in Fig. 4, the SERRS spectrum can be represented by four Gaussians with rather high accuracy, whereas the Raman–RL spectrum is poorly fitted by four components. To achieve comparable accuracy, the Raman–RL spectrum must be fitted with nine Gaussians, which demonstrates that it comprises more features. A detailed comparison shows that the features observed only in the Raman–RL spectrum are also present (poorly resolved) in the SERRS spectrum, which can be interpreted as additional evidence that they do exist.

Further evidence that the Raman–RL spectrum is more structured is that almost all its lines have counterparts in the IR absorption spectrum of R6G [13] (Fig. 5). (For comparison, the absorption spectrum in Fig. 5 is displaced to the visible region and converted, like the SERRS spectrum above, to wavelengths $\lambda = (\nu_e - \nu_{ir})^{-1}$, where ν_{ir} is the IR absorption frequency.) Note that the same refers to the lines that were missing in the SERRS spectra but were detected in the Raman–RL spectrum, as illustrated by the example of the weak lines at

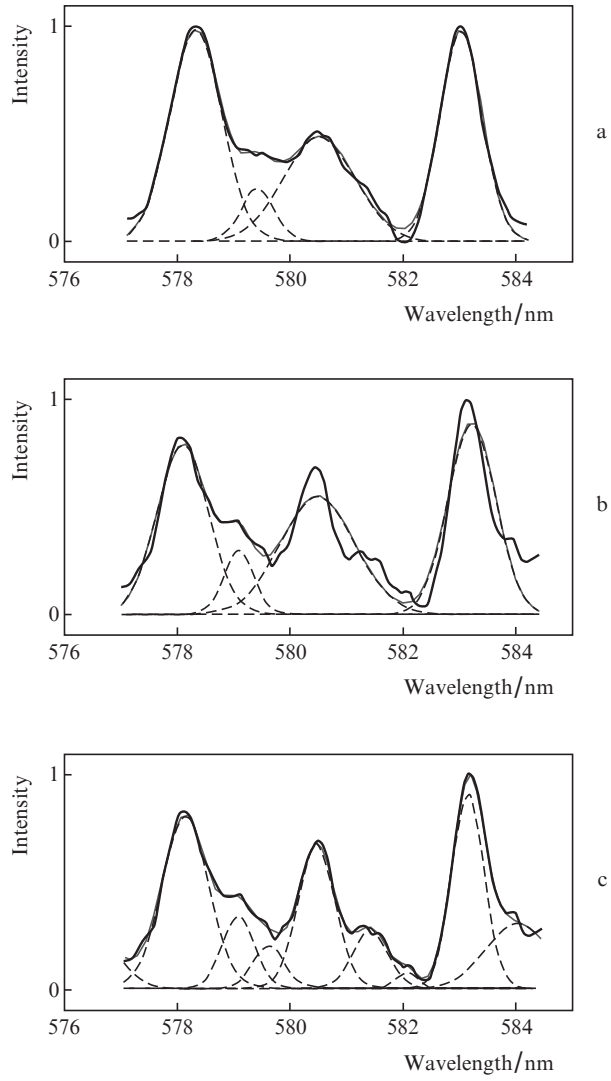

Figure 4. Portions (λ = 577–584 nm) of the (a) SERRS [1] and (b, c) Raman–RL spectra of R6G decomposed into (a, b) four and (c) nine Gaussian components. The thick solid lines show the measured spectra, the dashed lines show the Gaussian components, and the thin solid lines represent the fits with the Gaussians.

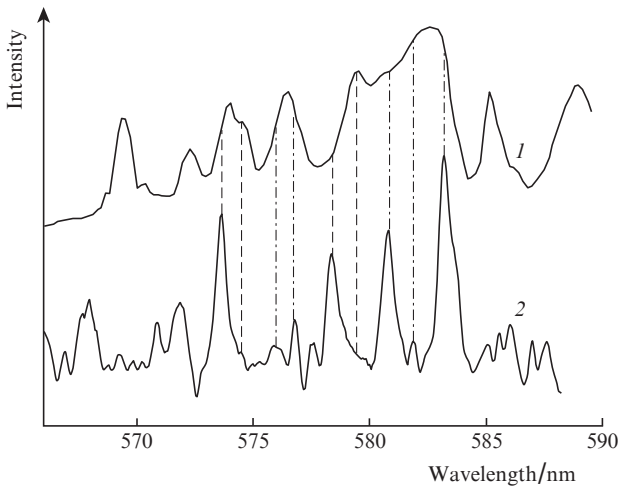

Figure 5. Comparison of (*2*) the Raman–RL spectrum of R6G to (*1*) its IR absorption spectrum [13].

574.5 and 579.4 nm, which were situated on the long-wavelength wings of the strong lines at 573.6 and 578.4 nm. Because different selection rules apply to IR absorption and Raman scattering, their spectra differ in the relative intensities of lines, and weak Raman lines may have stronger counterparts in the IR spectrum, which would confirm their existence.

The higher degree of structuring of the Raman–RL spectrum can in turn be used to reveal the hidden structure of individual IR absorption bands, which is at best only slightly discernible. This can be exemplified by the broad IR absorption bands centred at 576.4 and 582.6 nm: according to the Raman–RL spectrum, these are a doublet (576.0 and 576.8 nm) and a triplet (580.8, 581.8, and 583.2 nm).

Comparison of the SERSS and Raman–RL spectra leads us to conclude that the larger number of features in the latter is due not to changes in the relative intensity of spectral lines but to their narrowing and the formation of deep troughs between them. Raman lines are separated by sharp dips, which most likely result from the aforementioned interference between SRS and ASE over a photon mean free path in the medium. A similar situation occurs in CARS, where the resonant component (due to vibrations of molecules) interferes with the nonresonant component (due to electrons) of stimulated scattering [4]. This leads to an unusual spectral dependence of scattered intensity, with a sharp dip on the wing of a Raman line, which 'tones' it off on one side. As a result, when two Raman–RL lines approach one another, they do not merge and are separated by a sharp dip. One of the strongest lines in the Raman–RL spectrum of R6G (at 573.6 nm), marked by a dot-dashed line in Fig. 3, has precisely such a structure.

An important point is that vibrations of the matrix (a polymer in this study) containing an organic dye do not show up in Raman–RL spectra. This is due to the resonant nature of SRS: the pump wavelength lies in an absorption band of the dye, so the SRS probability for the dye molecules exceeds that for the matrix even though the concentration of polymer molecules is much higher (by three orders of magnitude). This is so provided that the matrix is transparent to pump light, meaning that it produces no resonance conditions for SRS from its molecules. Otherwise, its vibrations may show up in the Raman–RL spectrum.

Requirements for the matrix are not limited to its transparency and the ability of the dye to dissolve in it because, as a result of interaction between dye and polymer molecules, the matrix may influence the frequency of particular modes of the dye [14]. This interaction may change vibrational frequencies by up to several tens of reciprocal centimetres, so one should use as inert a matrix as possible or carefully analyse results.

The same method was used to obtain the Raman spectrum of P920 in the range 1200–1500 cm^{-1}, which showed up in the RL spectrum between 569 and 578 nm. Figure 6 shows RL spectra of this dye at two pump intensities and the Raman–RL spectra derived from them. With increasing pump intensity, the ASE band shifts to longer wavelengths and, in accordance with the above mechanism, increases the intensity of the lines that fall in its spectral range. This behaviour of the intensity is characteristic of SRS combined with stimulated emission in a single nonlinear process [6].

As follows from the mechanism of the phenomenon and Eqn (3), the Raman–RL spectrum is independent of the RL spectrum and the shape of its continuous component. Therefore, the discrepancy between the Raman–RL spectra in Fig. 6c, derived from different RL spectra, can be considered the

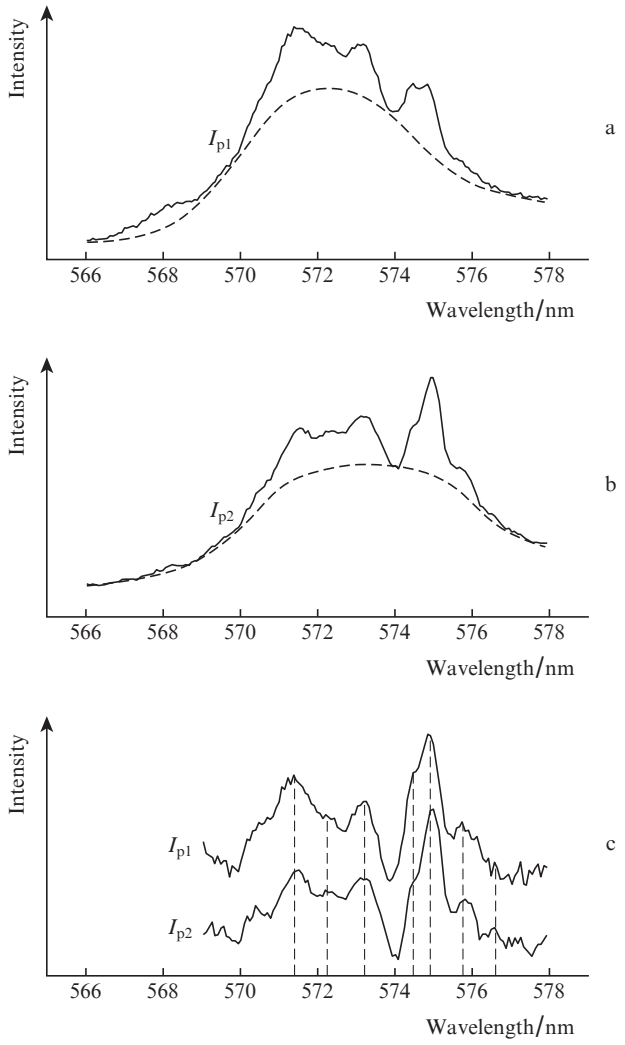

Figure 6. (a, b) RL (solid lines) and ASE (dashed lines) spectra of P920 at two pump intensities ($I_{p2} > I_{p1}$) and (c) Raman–RL spectra derived from them.

result of insufficient accuracy. From this viewpoint, accurate determination of the shape of the continuous component is critical because it influences the accuracy in the Raman–RL spectrum.

The spectral shape of the continuous component is rather difficult to find because it is governed by ASE and, hence, depends on the effective gain coefficient k_{eff} (which is a function of λ) and photon mean free path $\bar{l}$ in the MS medium. As a result, there is essentially no universal shape of this component because $k_{eff}(\lambda)$ and $\bar{l}$ are in turn dependent on many parameters of the medium. In particular, $k_{eff}(\lambda)$ is determined by the inversion density, which depends on the pump intensity, dye concentration and loss coefficient, and $\bar{l}$ is determined by the efficiency of light scattering from the embedded particles (vesicles), which depends on their concentration and relative index of refraction and the dimensions of the sample. To evaluate these parameters, one has to solve an intricate, multiparametric problem of modelling light propagation in an MS medium, which may nullify the advantages of the method in question.

This difficulty can however be obviated by utilising the requirement that the Raman–RL spectrum be independent of the RL spectrum in order to minimise the above-mentioned uncertainty in determination of the Raman–RL spectrum. The problem then reduces to batch processing of N RL spectra that gives N Raman–RL spectra differing very little from each other. This allows one to design an algorithm and software for automatically finding the shape of the continuous component in the RL spectrum that would minimise the deviation of the N Raman–RL spectra from the average, which will be the sought spectrum.

As seen in Fig. 6, the Raman–RL spectrum of P920 contains at least five Raman lines in the range 569–578 nm, with Raman shifts from 1200 to 1500 cm^{-1} (Table 1). According to previous work [15, 16], it is this region that contains vibrational frequencies of the C–C and CH_3-N^+ single bonds and deformation frequencies of some atomic groups in the P920 molecule.

Table 1. Raman lines and shifts in the spectra of P920 and R6G.

Dye	Lines in the Raman–RL spectrum/nm	Raman shift/cm^{-1}
P920	571.5, 573.2, 575.0, 575.9, 576.6	1299, 1351, 1406, **1433**, **1454**
R6G	571.0, 571.9, 573.6, 575.9, 576.8	1284, 1311, 1369, **1433**, **1460**

In this context, it is of interest to compare the Raman shifts derived from the Raman–RL spectrum of P920 with those for the corresponding spectral region in the Raman–RL spectrum of R6G (Table 1). Both spectra contain two Raman lines (indicated by bold type) with identical (within the width of the instrumental function of our measurement system, 0.3 nm) Raman shifts: ν = 1433 and 1454 (1460) cm^{-1}. Clearly, these frequencies arise from vibrations of identical bonds or atomic groups in the two molecules. In particular, according to previous work [16, 17], 1460 cm^{-1} is the characteristic bending frequency of the CH_3 group, which is present in both molecules (Fig. 1). The coincidence of the frequencies suggests that the obtained Raman spectrum of P920 is quite accurate and that the described method is effective in determining Raman–RL spectra.

4. Conclusions

The present results demonstrate that Raman spectra of laser dyes can be determined with certainty from the spectra of their RL in MS active media. Based on the notion of the mutual influence of stimulated scattering and emission processes in RL, we derived an expression describing the Raman–RL spectrum. This allowed us to develop a technique for obtaining spectra, which was successfully tested for the well-known dye R6G and was used to determine for the first time the Raman spectrum of the laser dye P920.

The Raman–RL spectrum shows more features in comparison with Raman spectra obtained by other techniques, which is due to the formation of sharp dips between neighbouring lines owing to the interference between the scattered light (SRS) and amplified spontaneous emission. An important point is that the strong luminescence of the dye, which is a serious obstacle to spontaneous Raman scattering measurements, is here a favourable factor because it initiates RL. This allows Raman scattering to be observed in the Stokes region, facilitating the measurement procedure.

The present results lead us to conclude that determining Raman spectra from RL spectra is a potentially attractive

approach which is easier to implement and provides more detailed information in comparison with other methods.

References

1. Zeng-Hui Zhou, Li Liu, Gui-Ying Wang, Zhi-Zhan Xu. *Chin. Phys*., **15** (1), 126 (2006).
2. Meixner A.J., Vosgrone T., Sackrow M. *J. Lumin.*, **94-95**, 147 (2001).
3. Lau A., Vernike V., Pfeifer M., et al., *Kvantovaya Elektron*., **3**, 739 (1976) [*Sov. J. Quantum Electron.*, **6**, 402 (1976)].
4. Akhmanov S.A., Koroteev N.I. *Metody nelineinoi optiki v spektroskopii rasseyaniya sveta* (Nonlinear Optical Methods in Light Scattering Spectroscopy) (Moscow: Nauka, 1981) pp 153–1163.
5. Yashchuk V.P., Tikhonov E., Prygodiuk O., Koreniuk V., Paskal L. *Proc. SPIE–Int. Soc. Opt. Eng.*, **6728**, 67280N1 (2007).
6. Yashchuk V.P., Tikhonov E.A., Prigodyuk O.A. *Pis'ma Zh. Eksp. Teor. Fiz*., **91** (4), 174 (2010).
7. Letokhov V.S. *Zh. Eksp. Teor. Fiz.*, **4** (10), 1442 (1967).
8. Wiersma D.S. *Nat. Phys.*, **4**, 359 (2008).
9. Cao H. *Lasing in random media. Waves random media*, **13**, R1 (2003).
10. Lawandy N.M., Balachandran R.M., Gomes A.S.L., Saurvain E. *Nature*, **368**, 436 (1994).
11. Yashchuk V.P., Tikhonov E.A., Prygodiuk O.A. *Mol. Cryst. Liq. Cryst*., **535**, 156 (2011).
12. Bobovich Ya.S., Bortkevich A.V. *Usp. Fiz. Nauk*, **103** (1), 3 (2009).
13. http:// riodb01.ibase.aist.go.jp/sdbs/cgi-bin/direct_frame_top.cgi.
14. Abd El Mongy S. *Aust. J. Basic Appl. Sci*., **3** (3), 1954 (2009).
15. El'yashevich M.A. *Atomnaya i molekulyarnaya spektroskopiya* (Atomic and Molecular Spectroscopy) (Moscow: Fizmatgiz, 1962) pp 714–717.
16. Bellamy L.J. *The Infra-Red Spectra of Complex Molecules* (London: Wiley, 1958; Moscow: Inostrannaya Literatura, 1958) pp 33–34.
17. Banwell C.N. *Fundamentals of Molecular Spectroscopy* (New York: McGraw-Hill, 1983; Moscow: Mir, 1985) pp 123–125.